Thermo-mechanical modelling of materials containing micro/nano inclusions with imperfect interfaces

J. Yvonnet[1], H. Le-Quang[1], C. Toulemonde[2], Q.-C. He[1]

[1]Université Paris-Est - 5 Bd Descartes, F-77454 Marne-la-Vallée cedex 2, France
e-mail: jyvonnet@univ-mlv.fr
[2]EDF - Site des Renardières - Avenue des Renardières - Ecuelles, F-77818 Moret sur Loing Cedex, France

ABSTRACT: In the present work, we present an efficient numerical procedure to compute the effective properties of materials containing micro and nano particles with imperfect interfaces. Firstly, a contiuum framework is proposed to model the size effect occuring in nanomaterials. For this purpose, we use the imperfect coherent interface model based on the Laplace-Young equation. Secondly, we model imperfectly bonded particles using the spring layer model. Both models are implemented through a combined XFEM/Level-set method, that allows modelling the different heterogeneities with arbitrary shapes and distributions through regular meshes. Even though this study is concerned with material analysis, it provides the basis for the introduction of particles with imperfectly bounded interfaces in forming processes analysis, e.g. in polymer injection including nano/coated particles.

KEYWORDS: Nanomaterials, Imperfect interfaces, XFEM, Level-set

1 INTRODUCTION

Modelling materials containing imperfectly bounded inclusions is of fundamental interest. On one hand, it has been shown that surface effects which are dominant at the nanoscale can be accurately modelled in a continuum framework by an imperfect coherent interface [2]. On the other hand, thin interphases which can be found in coated particles/fibres composites or in concrete materials can be modelled by an imperfect interface using the spring layer model. Owing to the fact that the surface energy can no longer be neglected when the interfaces are imperfect and due to the non-constant volume/surface ratio, the effective properties of such materials are size-dependent. In the present work, we present weak formulations for the different models, which are discretized with the extended finite element method [1]. The interfaces are modeled using a level-set function, which allows constructing the appropriate projectors needed to construct surface operators and appropriate discontinuous functions within the XFEM. The proposed framework permits computing effective properties of materials containing inclusions with arbitrary shapes or inclusions. Both thermal and mechanical cases are treated.

2 COHERENT IMPERFECT INTERFACE MODEL

2.1 Elastic formulation

We consider a domain $\Omega^{(1)}$ containing inclusions that are denoted collectively as $\Omega^{(2)}$. Both domains are separated by an interface Γ, that is assumed to be an imperfect coherent one in the present case. The equilibrium equations are given by

$$\mathbf{div}(\boldsymbol{\sigma}^{(i)}) = \mathbf{0} \;\; in \;\; \Omega^{(i)} \;, \; i = 1, 2 \;, \tag{1}$$

$$\mathbf{div}_s \boldsymbol{\sigma}_s = -[[\mathbf{t}]] = (\boldsymbol{\sigma}^{(2)} - \boldsymbol{\sigma}^{(1)})\mathbf{n}^{(1)} \;\; on \; \Gamma \;, \tag{2}$$

where $\mathbf{n}^{(i)}$ is the unit normal vector to Γ pointing into $\Omega^{(i)}$ and $\mathbf{div}_s(.)$ is the surface divergence operator defined by

$$\mathbf{div}_s(\mathbf{T}) = \nabla(\mathbf{T}) : \mathbf{P} \;, \tag{3}$$

where $\mathbf{P}$ characterizes the projection on the plane tangent to Γ at $\mathbf{x}$ and is defined by

$$\mathbf{P}(\mathbf{x}) = \mathbf{I} - \mathbf{n}(\mathbf{x}) \otimes \mathbf{n}(\mathbf{x}). \tag{4}$$

The boundary conditions are described by

$$\begin{cases} \boldsymbol{\sigma}\boldsymbol{\nu} = -\mathbf{F} \;\; on \;\; \partial\Omega_F \;, \\ \mathbf{u} = \bar{\mathbf{u}} \;\; on \;\; \partial\Omega_u \;, \end{cases} \tag{5}$$

where $\boldsymbol{\nu}$ is the outward unit vector normal to $\partial\Omega$, $\mathbf{F}$ and $\bar{\mathbf{u}}$ are prescribed tractions and displacements, respectively, and $\partial\Omega_F$ and $\partial\Omega_u$ are the Dirichlet and Neumann boundaries, respectively. According to the coherent interface model, the displacement jump across Γ is null:

$$[[\mathbf{u}]] = \mathbf{0} \ \ on \ \ \Gamma \ , \tag{6}$$

while the strain tensor is discontinuous according to the Hadamard relation:

$$[[\boldsymbol{\epsilon}]] = \mathbf{a} \otimes \mathbf{n} + \mathbf{n} \otimes \mathbf{a} \ , \tag{7}$$

where $\boldsymbol{\epsilon}$ is the infinitesimal strain tensor, and $\mathbf{a}$ is a real-valued vector. Here we assume that the solid undergoes small displacements. In the context of a linear elastic model, the bulk constitutive law is given by

$$\boldsymbol{\sigma}(\mathbf{u}) = \mathbf{C}^{(i)} : \boldsymbol{\epsilon}(\mathbf{u}) \ , \tag{8}$$

where $\mathbf{C}^{(i)}$ is the fourth-order elastic stiffness tensor associated with domain $\Omega^{(i)}$. The surface stress $\boldsymbol{\sigma}_s$ is related to the surface-strain energy γ by the Schuttleworth's equation and leads to

$$\boldsymbol{\sigma}_s = \boldsymbol{\sigma}_0 + \mathbf{C}^s : \boldsymbol{\epsilon}_s \ , \tag{9}$$

where $\boldsymbol{\sigma}_0$ is a residual surface stress and

$$C^s_{ijkl} = \lambda_s P_{ij} P_{kl} + \mu_s \left(P_{ik} P_{jl} + P_{il} P_{jk} \right) \ . \tag{10}$$

The associated weak form is expressed by

$$\int_\Omega \boldsymbol{\epsilon}(\boldsymbol{\delta}\mathbf{u}) : \mathbf{C} : \boldsymbol{\epsilon}(\mathbf{u}) d\Omega + \int_\Gamma \mathbf{P}\boldsymbol{\epsilon}(\boldsymbol{\delta}\mathbf{u})\mathbf{P} : \mathbf{C}^s : \mathbf{P}\boldsymbol{\epsilon}(\mathbf{u})\mathbf{P} d\Gamma$$

$$= \int_\Omega \boldsymbol{\delta}\mathbf{u} \cdot \mathbf{b} d\Omega + \int_{\partial\Omega_F} \boldsymbol{\delta}\mathbf{u} \cdot \mathbf{F} d\Gamma + \int_{\partial\Gamma} \mathbf{P}\boldsymbol{\delta}\mathbf{u} \cdot \hat{\mathbf{F}} dl$$

$$+ \int_\Gamma \mathbf{P}\boldsymbol{\epsilon}(\boldsymbol{\delta}\mathbf{u})\mathbf{P} : \boldsymbol{\sigma}_0 d\Gamma \ . \tag{11}$$

More details can be found in [4].

2.2 Modelling of composite with highly conducting interface

We denote by $T^{(i)}$ and $\mathbf{q}^{(i)}$ the temperature and heat flux vector fields respectively over $\Omega^{(i)}$ ($i = 1, 2$). Since the interface Γ is highly conducting, the temperature field is continuous across Γ, i.e.,

$$[[T]] = T^{(2)} - T^{(1)} = 0 \ on \ \Gamma, \tag{12}$$

but the heat flux vector jumps across Γ, i.e.,

$$[[\mathbf{q}]] \cdot \mathbf{n} = (\mathbf{q}^{(2)} - \mathbf{q}^{(1)}) \cdot \mathbf{n} \neq 0 \ on \ \Gamma. \tag{13}$$

Within the framework of steady thermal conduction and in the absence of heat source, the bulk energy conservation equation reads

$$div\mathbf{q}^{(i)} = 0 \ in \ \Omega^{(i)}, \tag{14}$$

and the interface energy conservation equation takes the form

$$-div_s\mathbf{q}_s = (\mathbf{q}^{(2)} - \mathbf{q}^{(1)}) \cdot \mathbf{n} \ on \ \Gamma \ . \tag{15}$$

The materials forming the matrix and inclusions are assumed to comply with the Fourier law. Thus, the local thermal conduction law reads

$$\mathbf{q}^{(i)}(\mathbf{x}) = -\mathbf{K}^{(i)} \nabla T^{(i)}(\mathbf{x}) \ in \ \Omega^{(i)}, \tag{16}$$

where $\mathbf{K}^{(i)}$ is the thermal conductivity tensor of the material constituting the matrix ($i = 2$) or the inclusions ($i = 1$). In addition, we make the assumption that the thermal conduction of the imperfect interface Γ is also governed by the Fourier law:

$$\mathbf{q}_s(\mathbf{x}) = -\mathbf{K}_s \nabla_s T(\mathbf{x}) \ on \ \Gamma. \tag{17}$$

In this equation, $\mathbf{K}_s$ is the interface thermal conductivity tensor of Γ having the property that $\mathbf{K}_s = \mathbf{P}\mathbf{K}_s\mathbf{P}$ and $\nabla_s(\bullet)$ is the surface gradient operator given by

$$\nabla_s \theta = \mathbf{P} \nabla \theta \tag{18}$$

for any differentiable scalar field θ defined on Γ. The boundary conditions on $\partial\Omega$ are in general mixed:

$$\begin{cases} \mathbf{q} \cdot \boldsymbol{\nu} = -\bar{q}_\nu \ \ on \ \ \partial\Omega_q, \\ T = \bar{T} \ \ on \ \ \partial\Omega_T, \end{cases} \tag{19}$$

where $\bar{q}_\nu$ and $\bar{T}$ are the heat normal flux and temperature prescribed on $\partial\Omega_q$ and $\partial\Omega_T$, respectively. Within this framework the weak form then reads

$$\int_\Omega (\mathbf{K}^{(i)} \nabla T) \cdot \nabla(\delta T) d\Omega + \int_\Gamma (\mathbf{K}_s \nabla_s T) \cdot \nabla_s(\delta T) dS$$

$$= \int_{\partial\Omega_q} \bar{q}_\nu \delta T dS. \tag{20}$$

3 SPRING LAYER IMPERFECT INTERFACE MODEL

3.1 Mechanical formulation

To model thin interphase with low mechanical properties, the spring layer interface model is introduced. The interface conditions for the linear spring layer model can be written as:

$$[[\boldsymbol{\sigma}]]\mathbf{n} = \mathbf{0}\ , \quad \mathbf{K}^s[[\mathbf{u}]] = \boldsymbol{\sigma}\mathbf{n}\ . \tag{21}$$

In the above, $\mathbf{K}^s$ is a second order tensor defined as

$$\mathbf{K}^s = \alpha_n \mathbf{n}\otimes\mathbf{n} + \alpha_s \mathbf{s}\otimes\mathbf{s} + \alpha_t \mathbf{t}\otimes\mathbf{t} \tag{22}$$

where α_n, α_s and α_t represent the interface elastic parameters in the normal and tangential directions, respectively, and $\mathbf{s}$ and $\mathbf{t}$ represent two orhogonal unit vectors in the tangent plane of the interface. Within this model the following weak form is obtained:

$$\int_\Omega \boldsymbol{\sigma}(\mathbf{u}) : \boldsymbol{\epsilon}(\boldsymbol{\delta}\mathbf{u}) d\Omega + \int_\Gamma [[\boldsymbol{\delta}\mathbf{u}]] \cdot \mathbf{K}^s [[\mathbf{u}]] d\Gamma$$

$$= \int_{\partial\Omega_t} \bar{\mathbf{t}} \cdot \boldsymbol{\delta}\mathbf{u} d\Gamma \tag{23}$$

4 X-FEM/LEVEL-SET DISCRETIZATION

Wherever needed, the components of $\mathbf{n}(\mathbf{x})$ can be evaluated numerically by:

$$\tilde{\mathbf{n}}(\mathbf{x}) = \nabla\tilde{\phi}(\mathbf{x}) / \left\|\nabla\tilde{\phi}(\mathbf{x})\right\|\ , \tag{24}$$

where

$$\nabla\tilde{\phi}(\mathbf{x})_i = \sum_{j=1}^{n} \frac{\partial N_j(\mathbf{x})}{\partial x_i}\phi_j\ . \tag{25}$$

Here $N_j(\mathbf{x})$ are the standard finite element shape functions, ϕ_j are the nodal value of the level-set function, and n is the number of nodes of the elements.

For the coherent interface model, the displacements must be continuous at the interface whereas the strains must follow the Hadamard relation described in Eq. (7). In the spring layer model, the displacements must be discontinuous at the interface while the stresses are continuous according to Eq. (21). These conditions can be enforced by superposing to the standard finite element field an enrichment term that possesses the above continuity conditions (XFEM method [1]). In this context, the approximation is defined at a particular point $\mathbf{x}$ lying in an element Ω_e by:

$$\mathbf{u}^h(\mathbf{x}) = \sum_{i=1}^{n} N_i(\mathbf{x})\mathbf{u}_i + \sum_{j=1}^{m} N_j(\mathbf{x})\psi(\mathbf{x})\mathbf{a}_j\ . \tag{26}$$

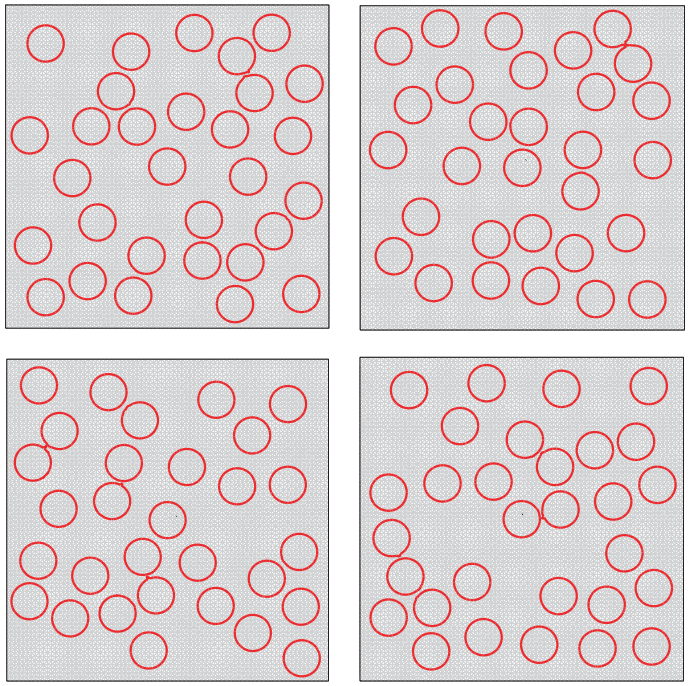

Figure 1: Level set function for the different randomly distributed nanopores.

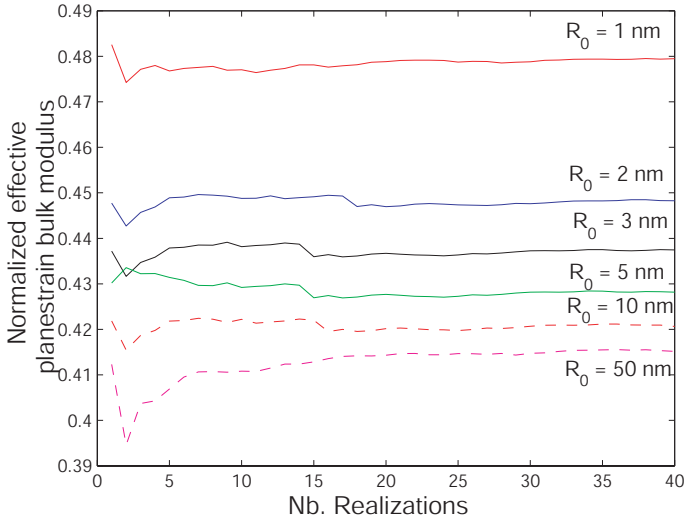

Figure 2: Statistical convergence of the effective bulk modulus for various void radii.

5 NUMERICAL EXAMPLES

5.1 Random nanostructure

In this example we explore the effective properties of aluminium containing randomly distributed nanopores with constant radii, in order to investigate its size-effects on effective properties. For this purpose, we use 30 circular voids randomly distributed, by choosing the size of the square domain such that the volume fraction is $f = 0.3$, and we vary the radius of the pores. A uniform mesh of 80×80 nodes is used (see figure 1), and an appropriate level-set function is chosed to describe the interfaces [4]. An Example of statistical convergence are shown in figure 2. The size effects with different nanovoid radii can be clearly observed.

5.2 Shape effects on the thermal effective properties of nanocomposites

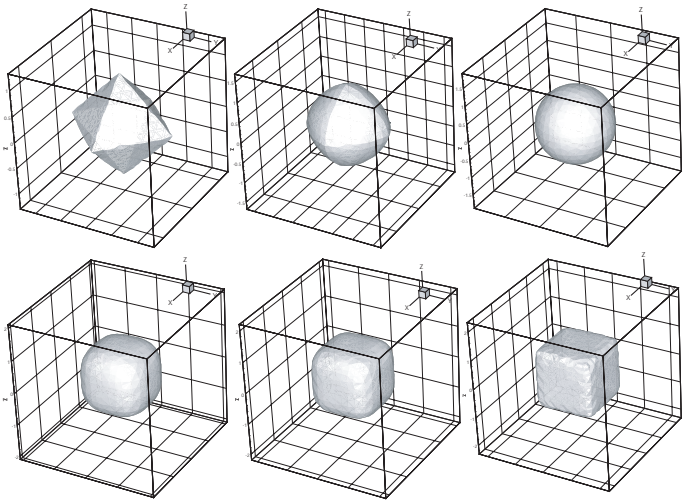

Figure 3: Inclusions of different shapes and with the same volume fraction $f = 0.1$.

In this example we use our procedure to evaluate the shape effects on the effective conducting properties of a nanocomposite. Using an appropriate level-set function, different shapes are generated at constant volume fraction (see figure 3). We note (see figure 4) that when no surface effects are considered, the optimal value of the effectivity is found for a spherical shape. In contrast, for $k_s > 0$ higher values for the effective conductivity can be obtained for some other shapes.

6 CONCLUSIONS

In this work, weak formulations have been established which are suitable for the numerical computation of the effective properties of a particulate composite in which the inclusions have different sizes, arbitrary shapes and imperfect interfaces. An extended finite element method has then been used in tandem with a level-set technique to elaborate an efficient numerical procedure for modelling imperfect curved interfaces without resort to curvilinear coordinates and surface elements.

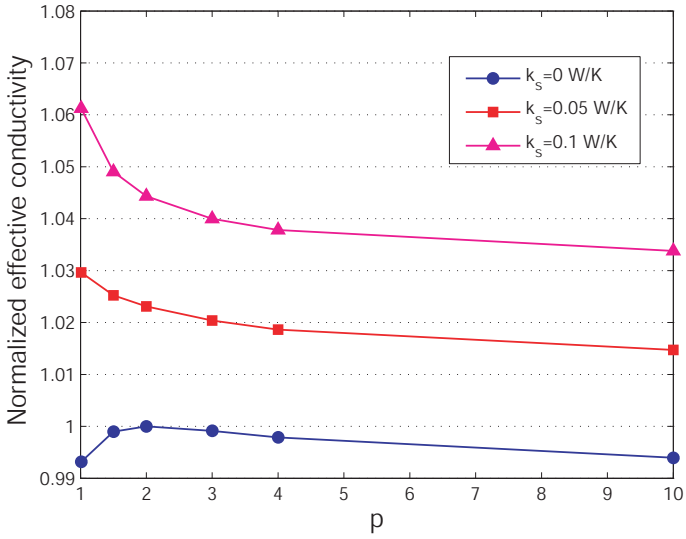

Figure 4: Effects of shape and surface conductivity on the effective conductivity, $f = 0.1$.

ACKNOWLEDGEMENT

The support this work enjoys from EDF is greatly aknowledged.

REFERENCES

[1] T. Belytschko and T. Black. Elastic crack growth in finite elements with minimal remeshing. *Int. J. Numer. Methods Eng.*, 455(5):601–620, 1999.

[2] H.L. Duan, Z.P. Wang, and B.L. Karihaloo. Size-dependent effective elastic constants of solids containing nano-inhomogeneities with interface stress. *J. Mech. Phys. Solids*, 53(7):15741596, 2005.

[3] J. Yvonnet, Q.-C. He, and C. Toulemonde. Numerical modelling of the effective conductivities of composites with arbitrarily shaped micro- or nano-inclusions and highly conducting interface. *Composites Sc. Tech., submitted*.

[4] J. Yvonnet, H. Le Quang, and Q.-C. He. An xfem/level set approach to modelling surface/interface effects and to computing the size-dependent effective properties of nanocomposites. *Comput. Mech., accepted*.